Synthesis and Structure of Nylons 1,*n*

Lourdes Franco, Eloísa Navarro, Juan A. Subirana, and Jordi Puiggalí*

Department d'Enginyeria Química, ETS d'Enginyers Industrials, Universitat Politècnica de Catalunya, Diagonal 647, Barcelona 08028, Spain

*Received February 7, 1994; Revised Manuscript Received April 26, 1994**

ABSTRACT: We have synthesized and characterized a series of copolymers of diaminomethane and α,ω-dicarboxylic acids (nylons 1,*n* with *n* = 5, 6, 7, 8, 10, and 12). Their structure has been determined by various methods, including X-ray diffraction and electron microscopy. A new conformation, different from conventional polyamides, has been found. It shows a characteristic shortening of the molecular repeat distance. When *n* is even, the polymers crystallize in a monoclinic system, space group $B2/b11$, whereas when *n* is odd, they crystallize in an hexagonal lattice, space group $P3_212$. A characteristic gauche conformation of the monomethylene bisamide units is in full agreement with all experimental results. The two amide groups in each unit are oriented in opposite directions. Structural differences in the series are explained in terms of conformational changes of the dicarboxylic unit depending on the number of methylene groups.

Introduction

The structure of synthetic polyamides (nylons) has been extensively studied by several authors. It has been shown that polyamides exist in various crystalline forms, α, β and γ,[1,2] depending on the number of methylene units,[3,4] conditions of crystallization,[5] and also on processing[6] and treatment by iodine solutions.[7] All these well-established structures are based on parallel sheets which are stabilized by hydrogen bonds running in a single direction.

We have recently studied different nylons characterized by a close disposition of the amide groups –CONH– in the molecular chain, with a single methylene group between neigboring amide units. This is also characteristic of natural polyamides (proteins) and polypeptides which may adopt several helical conformations.[8] New structures with two or three hydrogen bond directions have been found in our laboratory in nylons 2/*n* (copolymers of glycine and ω-amino acids)[9–13] and *n*,3 (copolymers of α,ω-diaminoalkanes and malonic acid).[14–16] The isotropic distribution of hydrogen bonds will undoubtedly influence the properties of these polymers.

The copolymers of diaminomethane and α,ω-dicarboxylic acids (nylons 1,*n*) are another family of polymers which also have an isolated methylene group between amide groups. Although their synthesis by condensation of formaldehyde with difunctional nitriles is known,[17] no systematic structural study has been carried out with these polymers. Furthermore, X-ray studies of model molecules as bis(acetamido)methane point to a new conformation around the isolated methylene group, which could induce its two neighbor amide groups to orient themselves in exactly opposite directions.[18] Quantum mechanical calculations also confirm that this new conformation is energetically favored.[19] Therefore we decided to study in more detail this family of polymers. Some results on nylons 1,3[20] and 1,4[21] have already been reported. A 3-fold helical conformation and a layered structure have been respectively found showing conformational differences depending on the number of methylene groups in the dicarboxylic unit. In the present work we describe the structure of several nylons 1,*n* with *n* even (6–12) and also some polymers with *n* odd (5 and 7). Since side reactions during the polymerization with formaldehyde may be produced, we gave special attention to polymer characterization. Also a new method of synthesis was used for nylon 1,7, since these polyamides cannot be obtained by the conventional method of heating a dibasic acid and a diamine due to the fact that monomethylenediamine is unstable in the free state.[22]

Experimental Section

Synthesis and Characterization. All chemicals were ACS grade or higher and were used as received. Solvents were purified and dried by appropriate standard methods.[23] Polymers were prepared by the reaction of formaldehyde (paraformaldehyde) and the appropriate dinitrile according to Magat et al.[17] As it has been described,[24] the polymer properties depend on a large number of variables such as reaction time, temperature, nature of the acid used as catalyst, concentration, and molar balance of reactants. Preliminary studies showed[25] that side reactions were minimized when the polymerization was carried out at 0 °C. An equimolar proportion of reagents was used in order to minimize side reactions. Reaction times were optimized according to intrinsic viscosity measurements. The operation procedure consists in a slow addition with stirring of a half-volume of concentrated sulfuric acid over a 1 M solution of reagents in 90% formic acid. Polymers were recovered from the reaction mixture by precipitation with four volumes of cold water. Low molecular weight impurities were removed by exhaustively washing with water, ethanol, and ethyl ether.

Nylon 1,7 was also synthesized by interfacial polycondensation of pimeloyl dichloride and *N,N'*-bis(aminomethyl)pimeloamide dichlorohydrate according to the method reported for nylon 6,-10.[26] The synthesis of the monomer *N,N'*-bis(aminomethyl)-pimeloamide dichlorohydrate was performed by applying the widely known methodology developed for the preparation of retro-inverse peptides[27] (Scheme 1). This monomer was purified by precipitation with HCl from a dioxane solution and its structure assessed by IR and NMR spectroscopies and elemental analysis (Found: C, 37.2; H, 7.7; N, 19.5. Calcd for $C_9H_{22}O_2N_4Cl_2$: C, 37.4; H, 7.6; N, 19.4). In order to prepare the polymer, approximately 10 mmol of the dichloride was dissolved in 100 mL of dry carbon tetrachloride and 10 mmol of the dichlorohydrate in 30 mL of 1.4 M sodium hydroxide solution was poured on top of it. The polymer did not readily form a rope and was isolated from a stirred mixture by filtration. It was washed successively with water, ethanol, and acetone and was kept in a vacuum desiccator at 60 °C.

The intrinsic viscosity of the polymers was determined with a Cannon-Ubbelohde microviscometer at a temperature of 25.0 ± 0.1 °C. Dichloroacetic acid was used as a solvent. The density of powder samples was measured at 25 °C by the flotation method in mixtures of ethanol and carbon tetrachloride.

Infrared absorption spectra were recorded from potassium bromide pellets with a Perkin-Elmer 783 spectrophotometer in the 4000–500-cm^{-1} range. NMR spectra were registered from polymer solutions in deuterated trifluoroacetic acid using a Bruker

* Abstract published in *Advance ACS Abstracts*, June 1, 1994.

0024-9297/94/2227-4284$04.50/0

Scheme 1

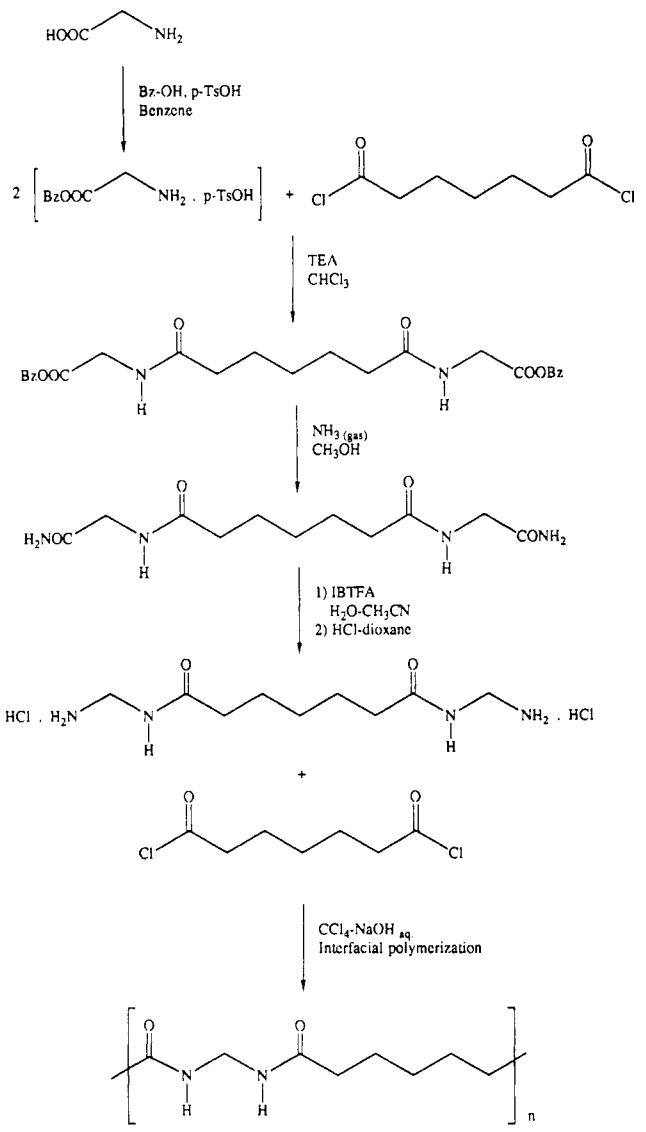

ABBREVIATIONS:

p-TsOH: para-toluenesulfonic acid
Bz-OH: benzyl alcohol
TEA: triethylamine
IBTFA: [bis(trifluoroacetoxy)iodo]benzene

AMX-300 spectrometer operating at 300.1 MHz for ^{1}H NMR and at 75.5 MHz for ^{13}C NMR. All cited chemical shifts are referred to tetramethylsilane (TMS) used as an internal standard.

Thermal behavior was investigated with a Perkin-Elmer DSC-4 equipped with a TADS data station at a heating rate of 10 °C/min in a nitrogen atmosphere. Temperature was calibrated using an indium standard. Thermogravimetry was carried out in a Perkin-Elmer TGS-1 analyzer at a heating rate of 10 °C/min.

Structural Methods. Crystallization experiments were carried out isothermally from dilute solutions (0.05–0.1% (w/v)) in polar polyfunctional alcohols such as 2-methyl-2,4-pentanediol (MPD) and 1,4-butanediol. The polymers were dissolved at 210 °C and the solutions were transferred to constant-temperature baths in the 50-140 °C interval for 2–5 h. Crystallization experiments were also carried out from dilute solutions of the polymers in mixtures of water and dichloroacetic acid between 70 and 98 °C. The crystals were recovered by centrifugation and were repeatedly washed with *n*-butanol.

For electron microscopy the crystals were deposited on carbon-coated grids which were then shadowed with Pt–carbon at an angle of 15°. A Philips EM-301 electron microscope operating at either 80 or 100 kV for bright field and electron diffraction modes, respectively, was used throughout this work. Electron diffraction diagrams were recorded by the selected area method on Kodak Tri-X films. The patterns were internally calibrated with gold (d_{111} = 2.35 Å). Polymer decoration was achieved by evaporating polyethylene onto the surface of single crystals, as described by Wittmann and Lotz.[28]

X-ray diagrams were recorded under vacuum at room temperature, and calcite (d_B = 3.035 Å) was used for calibration. A modified Statton camera (W. R. Warhus, Wilmington, DE) with Ni-filtered copper radiation of wavelength 1.542 Å was used for these experiments. Alternatively, a graphite monochromator was used in some experiments. Patterns were recorded from either polymer powders or from mats of single crystals which were prepared by slow filtration of a crystal suspension on a glass filter. We were unable to prepare oriented samples (films, fibers) from these polymers, probably due to the relatively low molecular weight.

The diffraction intensities were measured with a Joyce Loebl MK III CS microdensitometer and were corrected for area, Lorentz, and polarization factors (taking into account the modification of the usual formula due to the use of monochromator[29]). Structural modeling was achieved with the LALS methodology,[30] and calculations were run on a HP-340 computer.

Results and Discussion

Synthesis. The results obtained in the synthesis of the polymers are reported in Table 1. Since for structural studies regular polymers are required, we gave special attention to the polymerization conditions in spite of limiting the molecular weights. As it has been described,[24] an excess of formaldehyde produces cross-linked polymers probably due to side reactions that originate methylene bridges between amide nitrogens. ^{13}C-NMR spectra of polymers obtained at room temperature show evidence of chain branching. So we used an equimolar proportion of formaldehyde to dinitrile and a polymerization temperature of 0 °C. In all cases an optimum reaction time has been found, since depolymerization apparently occurs in the reaction medium. The optimum time increases as the methylene content of the dinitrile monomer increases, due to a lower reactivity. Intrinsic viscosities measured in dichloroacetic acid at 25 °C are between 0.18 and 0.23 dL/g for all polymers. The latter values indicate a low molecular weight, in fact a M_n between 1000 and 2000 can be estimated using the Elias and Schumacher equation derived for nylon 6,6.[31]

We have also used another method to prepare this family of polymers, starting from glycine and the appropriate diacyl chloride. The method is summarized in Scheme 1 and consists in a five-step synthesis which avoids the use of formaldehyde. Since the ideal monomethylenediamine monomer is unstable, we prepare a new monomer that incorporates aminomethanamide units. The synthesis starts by converting glycine to the benzyl ester using acid and benzyl alcohol. After the coupling with pimeloyl dichloride, we convert the glycine ester derivative to the amino–amide by adding ammonia. The *N,N'*-bis(aminomethyl)pimeloamide monomer is finally generated by employing a form of the Hoffmann rearrangement with *I,I*-bis(trifluoroacetoxy)iodobenzene (IBTFA). The monomer can be easily prepared in this way since each step has a high yield (75, 75, 93, and 95%, respectively). Interfacial polymerization with pimeloyl dichloride gives the polymer in 83% yield. No significant differences with the polymer obtained from formaldehyde synthesis are found, although the intrinsic viscosity is slightly higher (0.23 versus 0.19 dL/g). Attempts to increase the viscosity by either longer polymerization times or changes in monomer concentration failed. Intrinsic viscosity is probably limited by precipitation of the polymer during the course of polymerization.

Infrared Spectra. Infrared spectra of all polymers show characteristic amide and methylene absorption bands. These are summarized and compared in Table 2

Table 1. Synthesis and Characterization Data for Polyamides 1,*n*

polymer	react time (h)	yield (%)	elemental anal. (%) carbon calc	carbon found	hydrogen calc	hydrogen found	nitrogen calc	nitrogen found	$[\eta]^b$ (dL g^{-1})	$M_n{}^c$	$X_n{}^d$
nylon 1,5	0.5	75	50.70	48.76	7.04	6.79	19.72	18.85	0.18	2220	16.0
nylon 1,6	1.0	86	53.83	52.09	7.75	7.37	17.94	16.98	0.20	2180	14.3
nylon 1,7	1.0	88	56.47	56.78	8.24	8.21	16.47	16.41	0.19	1650	9.9
nylon 1,8	1.0	80	58.69	58.08	8.69	8.58	15.22	14.89	0.23	2350	13.0
nylon 1,10	2.5	84	62.26	61.57	9.43	9.17	13.21	12.85	0.18	1650	7.9
nylon 1,12	3.0	88	65.00	64.78	10.00	10.05	11.67	11.64	0.18	1390	6.0
nylon 1,7[a]	1.0	83	56.47	55.51	8.24	8.19	16.47	15.91	0.23	1900	13.5

[a] Synthesized by interfacial polymerization. [b] Intrinsic viscosity measured in dichloroacetic acid at 25 °C. [c] Determined from ^{1}H NMR spectroscopy. [d] Average degree of polymerization defined as the number of dicarboxylic units.

Table 2. Characteristic Infrared Bands (Wavenumber, cm^{-1}) of Nylons 1,*n* and Crystalline Forms of Nylon 6

polymer	amide A	amide B	CH_2 stretching asym	CH_2 stretching sym	amide I	amide II	CH_2 rocking	amide V	amide VI
nylon 1,5	3292	3055	2952	2868	1636	1538		704	582
nylon 1,6	3303	3056	2925	2855	1635	1536		698	577
nylon 1,7[a]	3297	3055	2922	2849	1636	1539	728[c]	697	572
nylon 1,8	3304	3064	2920	2848	1637	1541	721	694	578
nylon 1,10	3304	3060	2917	2846	1635	1540	721	696	576
nylon 1,12	3299	3061	2913	2843	1636	1539	721	694	577
N 6(α)[b]	3302	3062	2940	2868	1645	1550	731	690	580
N 6(γ)[b]	3302	3099	2940	2860	1651	1570	730		630

[a] No difference has been detected between polymers synthesized by condensation from formaldehyde and by interfacial polymerization. [b] Data of Abu-Isa.[32] [c] Appears as a shoulder.

with the infrared bands of α and γ forms of nylon 6.[32] In general the amide bands resemble the α-form in apparent disagreement with the X-ray evidence which will be presented below. This is most clear for the amide V and VI modes near 690 and 580 cm^{-1}, which occur at a position similar to that for the α-form, whereas the former peak is not seen for γ-crystals, while the latter peak shifts to 630 cm^{-1}. Methylene absorption intensities gradually increase, as expected, from nylon 1,5 to nylon 1,12 (Figure 1). However methylene stretching modes, with the exception of nylon 1,5, are clearly shifted from the values found in conventional forms. A very intense absorption band near 1120 cm^{-1} is characteristic for this family of nylons and might be related either to the weak C–C stretching mode reported for nylon 6 at 1121–1120 cm^{-1} or to skeletal motions involving amide groups reported as medium- and weak-intensity bands for γ- and α-forms, respectively, in the 1170–1070-cm^{-1} region. These puzzling features indicate a new structure for these nylons 1,*n*, as we will show in the following sections. On the other hand, a very weak nitrile absorption band at 2240 cm^{-1} is observed in polymers prepared from formaldehyde. This band is associated with terminal groups and confirms the low molecular weight of these polymers.

NMR Spectra and Molecular Weight Determination. The chemical shifts of the more intense signals observed in the ^{1}H and ^{13}C NMR spectra of nylons 1,*n* are reported in Table 3. All of them are in full agreement with the anticipated chemical composition. However signals attributed to terminal groups can also be observed and are consistent with nitrile end groups for the polymers synthesized from formaldehyde. The ^{1}H NMR spectra show a single signal for the monomethylene bis(amide) protons around 4.9 ppm, whereas the methylene protons next to the carbonyl groups appear between 2.6 and 2.7 ppm, generally as a resolved triplet with some weak overlapped signals which may be assigned to terminal groups. Furthermore integrated intensities show a deficit of monomethylene bis(amide) protons, specially for nylon 1,12 (Figure 2a). The observed relation can be explained from the low molecular weight of the samples if a nitrile

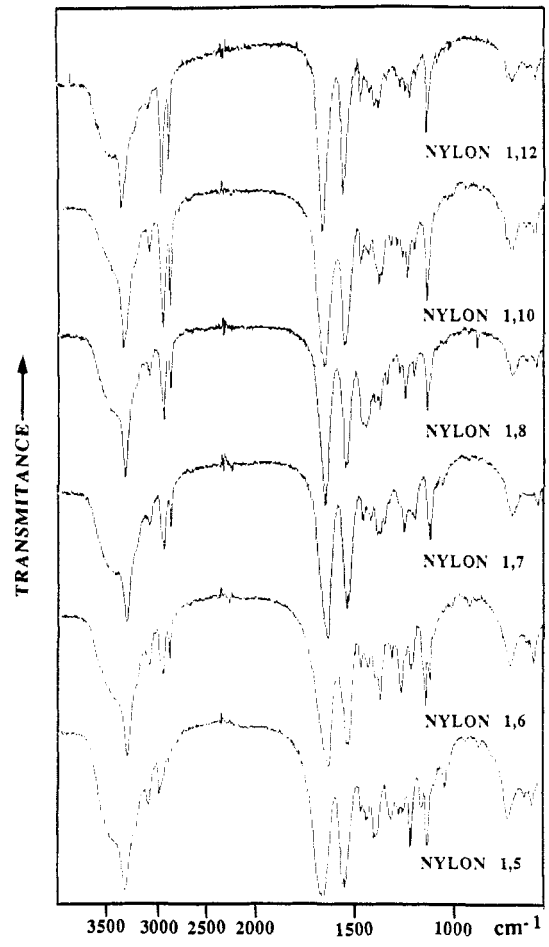

Figure 1. Infrared spectra of nylons 1,*n*.

group termination is assumed. So nylon 1,12, the compound with smallest molecular weight studied by us, has an average of five diamines and six diacid or equivalent units for an estimated 1400 molecular weight. In fact we can calculate the number average degree of polymerization x of the nylons 1,*n* with the expression: $x = p/[p - m(n$

Table 3. ^1H and ^{13}C Chemical Shifts of Nylons 1,*n*[a]

		a		b		c		d		e		f	
polymer	carbonyl	^{13}C	^1H	^{13}C	^1H	^{13}C	^1H	^{13}C	^1H	^{13}C	^1H	^{13}C	^1H
nylon 1,5	180.69	47.81	4.95	35.23	2.68	22.31	2.15						
nylon 1,6	181.70	47.91	4.94	35.89	2.62	26.09	1.85						
nylon 1,7	182.48	48.16	4.93	36.32	2.58	26.53	1.81	29.76	1.53				
nylon 1,8	183.05	48.25	4.93	36.45	2.57	26.82	1.77	29.83	1.47				
nylon 1,10	183.55	48.33	4.93	36.61	2.57	27.18	1.75	30.35	1.39	30.49	1.39		
nylon 1,12	183.73	48.34	4.93	36.66	2.57	27.36	1.74	30.60	1.37	30.60	1.37	30.80	1.37

[a] The polymers were dissolved in deuterated trifluoracetic acid. Tetramethylsilane was used as an internal reference. The methylene carbons are identified as shown in Figure 2.

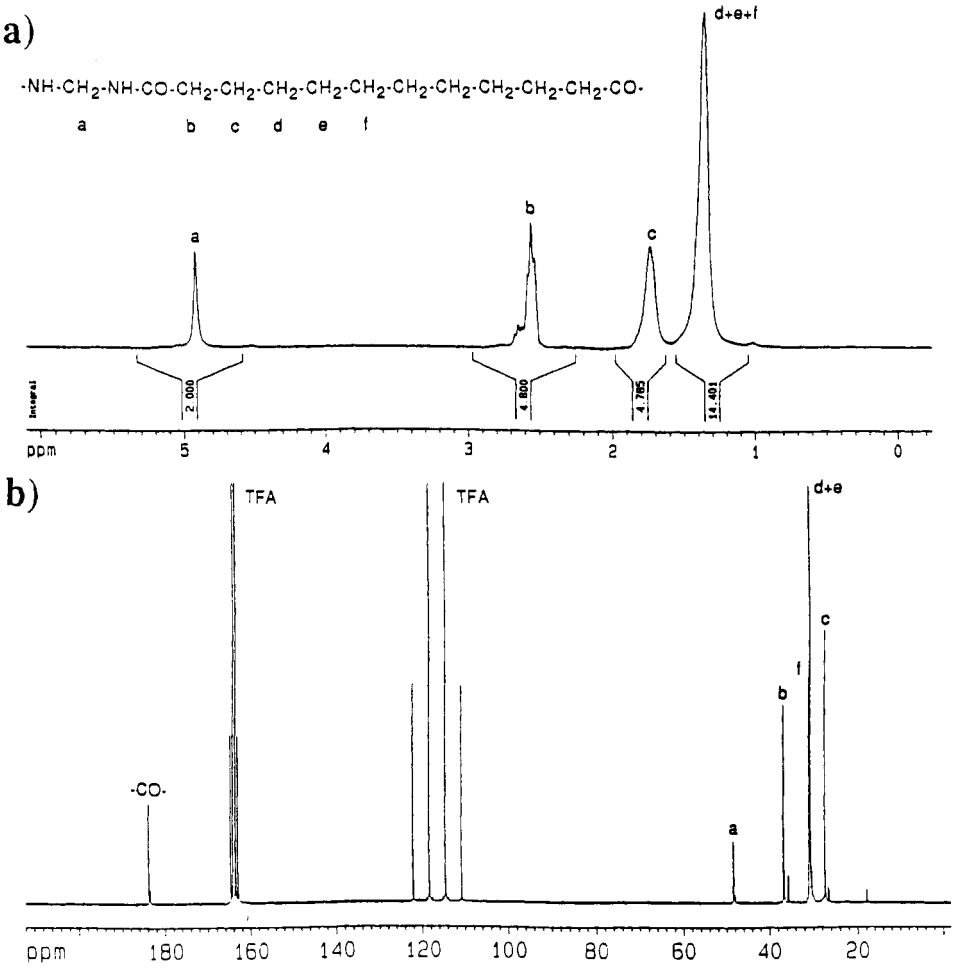

Figure 2. NMR spectra of a nylon 1,12 solution in deuterated trifluoroacetic acid: (a) ^1H; (b) ^{13}C. The other polymers show similar spectra. The minor side peaks in (b) are due to the terminal residues. The areas of proton signals are used to determine the molecular weight of the polymers, as discussed in the text.

$-2)]$, where m is the integrated area for protons in isolated methylenes and p is the integrated area for all protons in diacid units. x corresponds to the average number of diacid unit in each molecule. Since the terminal groups are the diacid units, the average number of methylene dipeptide units in each polymer is $(x-1)$. The resulting molecular weights are given in Table 1 and are always below 2500. The molecular weights determined in this way are significantly larger than those calculated from the intrinsic viscosity using an expression derived from nylon 6,6.[31] The difference is greater for smaller n values, whereas for nylon 1,12 the molecular weights determined with both methods are similar. It appears that a larger density of peptide groups (n small) results in a more compact conformation in solution of the low-molecular weight polymers studied by us. An intramolecular interaction of the peptide groups might contribute to this effect.

^{13}C-NMR spectra also present a single signal for the monomethylene bis(amide) carbons whereas the carbons of the dicarboxylic units show different signals in agreement with position effects (Figure 2b). Furthermore a signal around 18 ppm indicative of nitrile vicinal carbons is observed with variable intensity in all samples prepared from formaldehyde. The NMR spectra of nylon 1,7 synthesized by interfacial polymerization show similar characteristics.

Thermal Behavior. Figure 3 shows the DSC traces of solution-crystallized nylons 1,*n* with *n* odd, obtained at a heating rate of 10 °C/min. Data for the *n* even samples have recently been reported.[33] A single melting peak (nylon 1,5, 284 °C; nylon 1,6, 285 °C; nylon 1,8, 276 °C) or a multiple melting peak characteristic for nylons[34] (highest peak: 278 and 272 °C for nylon 1,7 prepared from formaldehyde and interfacial polymerization respectively; 266 °C for nylon 1,10; 259 °C for nylon 1,12) is observed. Unfortunately thermal decomposition starts during melting since a stable baseline is not reached after fusion. Moreover thermogravimetric measurements indicate that mass loss begins around 230–250 °C, always below the melting temperature, as shown in Figure 4. For instance

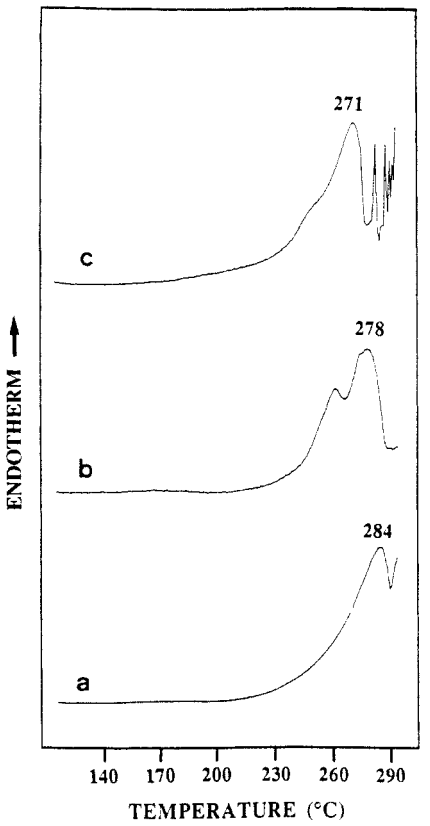

Figure 3. DSC for solution-crystallized nylons 1,*n* obtained at a rate of 10°/min: (a) Nylon 1,5 obtained from formaldehyde; (b) nylon 1,7 obtained from pimelonitrile and formaldehyde; (c) nylon 1,7 obtained by interfacial polymerization. The samples start to decompose during melting as shown in Figure 4.

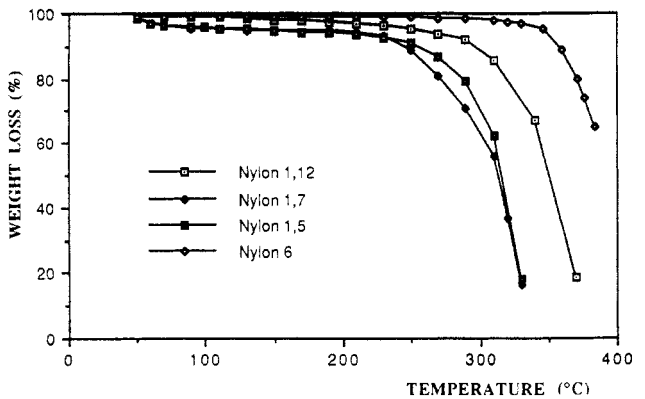

Figure 4. Thermogravimetry of nylons 1,12, 1,7, 1,5, and 6 given as weight loss as a function of temperature in °C.

thermogravimetry of nylon 1,12, which has the lowest melting point, already indicates a mass loss of 5% at the fusion peak temperature. The low decomposition temperatures appear as a distinctive characteristic for nylons 1,*n*. In Figure 4 we have also included nylon 6 for comparison. In this polymer decomposition starts at 307 °C, about 60 °C higher than in nylons 1,*n* and about 80 °C above its melting point.

As shown in Figure 5, a linear relationship between melting temperature and methylene number in a repeating unit chain has been found for nylons 1,*n* with *n* even, whereas *n* odd nylons have a slightly lower melting temperature. These results agree with literature values[35] where a linear relation is observed between melting temperature and hydrogen bond interactions for a given series of nylons. Nylons 1,5 and 1,7 slightly deviate from the correlation in the same way as nylons *m*,*n* differ according to the parity of *n* and *m*. However, due to the

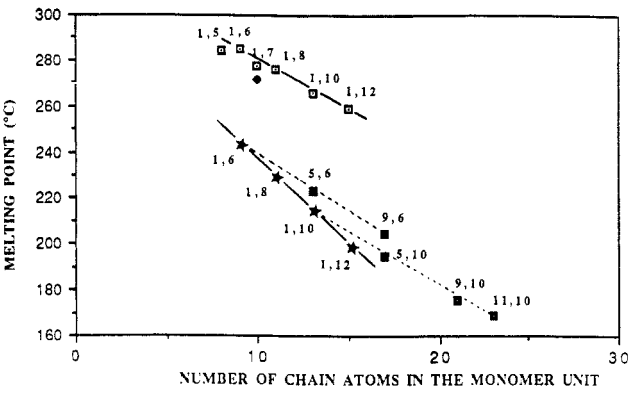

Figure 5. Melting points of polyamides versus number of chain atoms in the repeat unit: Experimental values for nylons 1,*n* synthesized from formaldehyde (⧈); experimental value for nylon 1,7 prepared by interfacial polymerization (◆). The values represented in the figure should be considered as lower limits, in particular for the smallest values of *n*, since decomposition accompanies melting as discussed in the text. The melting points for nylons 1,*n* (★) estimated by extrapolation from experimental data[36] for nylons *m*,*n* (■) are also shown. It is obvious that much lower melting points are obtained in this way.

low molecular weight of our samples and to the onset of the decomposition during fusion, the melting temperatures we report here represent lower limits. Furthermore differences are detected in thermal behavior between the two samples of nylon 1,7, probably due to differences in molecular weight and terminal groups. In all cases the melting temperatures are 40–60 °C higher than the values estimated by extrapolation from experimental data of polyamides[36] (Figure 5), probably due to the different organization of hydrogen bonds in this nylon family.

It is interesting to compare the melting points of these nylons with their isomers. The other two families of nylons (2/*n* and *n*,3), which also have an isolated methylene group between two peptide groups in the form of either glycine or malonamide, have similar melting points, as reported elsewhere.[15,33] The analogy among these three families of nylons is probably due to the similar conformation of the methylene–amide bond in all of them.[37] Apparently such conformation gives an enhanced structural stability to all these polymers.

The melting points of the nylons 1,*n* when compared with isomeric nylons *m*,*n* are higher, as discussed above (Figure 5). This difference is similar to that found between nylon 6,6 (T_m = 265 °C) and its isomer nylon 6 (T_m = 230 °C). Nylon 6 has a T_m similar to the nylons *m*,*n* shown in Figure 5, whereas nylon 6,6 has an anomalously high melting temperature. In fact it is striking that the melting temperature of nylon 6,6 falls exactly on line with the nylons 1,*n*. Such higher stability has been attributed to an enhanced mobility of the methylene groups in the solid state before melting,[38] a possibility which may be tentatively advanced as an additional explanation for the high melting points of the nylons 1,*n*, *n*,3, and 2/*n*.

Electron Microscopy. Nylons 1,*n* with *n* even crystallize from diol solutions as long sheaves with lath-shaped extremities (Figure 6a, nylon 1,6, and Figure 6d, nylon 1,12), as spindle-shaped multilayered crystals (Figure 6b, nylon 1,8), or as multilayered lath-shaped crystals (Figure 6c, nylon 1,10). The specific crystallization conditions used by us are summarized in Table 4. In all cases the crystals are about 50 Å thick as estimated from their shadows in the micrographs and confirmed by low-angle X-ray diffraction as reported below. Similar crystals had been previously obtained with nylon 1,4.[21] The crystals obtained from nylon 1,10 are larger, and they have well-

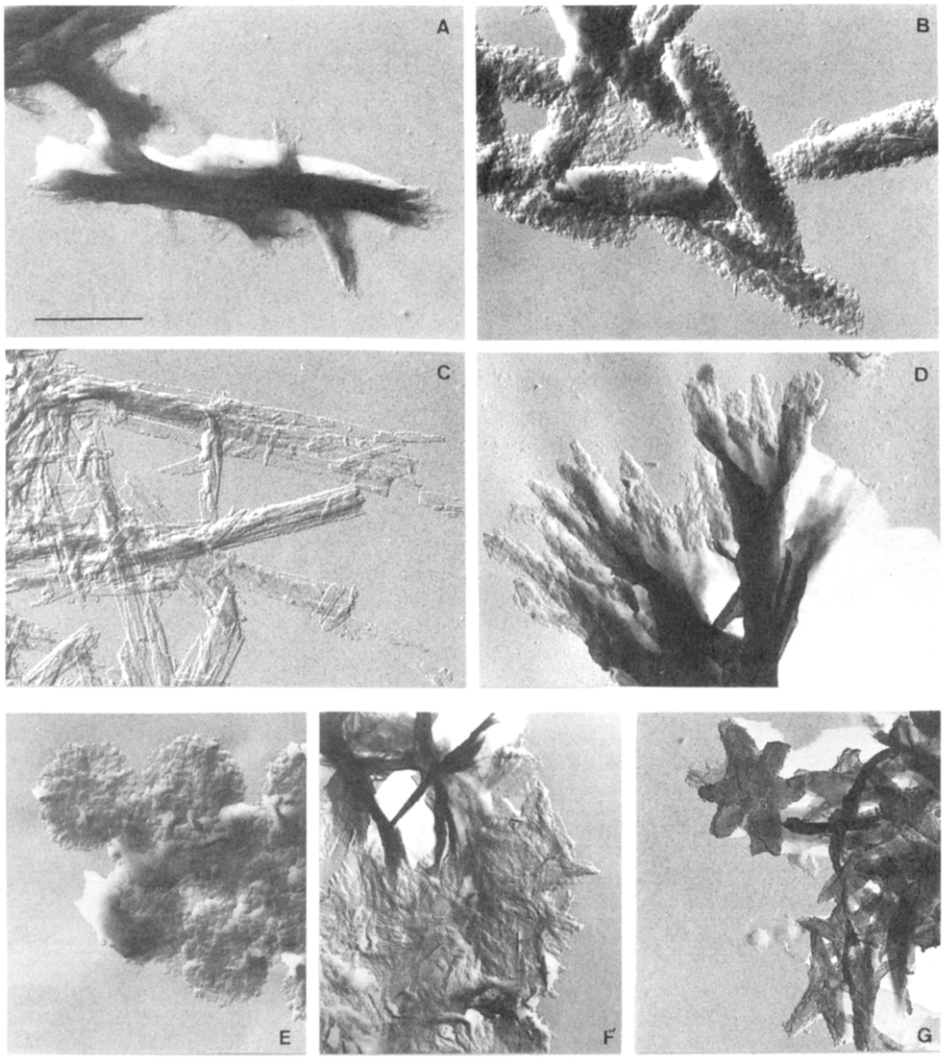

Figure 6. Transmission electron micrographs of crystals prepared in a diol solution of nylons (a) 1,6, (b) 1,8, (c) 1,10, (d) 1,12, and (e) 1,5. Electron micrographs of crystals prepared in a water–dichloroacetic acid solution of nylon 1,7 obtained from (f) formaldehyde and (g) interfacial polymerization. The conditions used in each case are given in Table 4. All micrographs are given at the same magnification (scale bar = 1 μm).

Table 4. Optimal Crystallization Conditions for Nylons 1,n

nylon	solvent	concn (mg/mL)	temp (°C)
nylon 1,6	1,4-butanediol	0.5	52
nylon 1,8	1,4-butanediol	1.0	58
nylon 1,10	2-methyl-2,4-pentanediol	1.0	70
nylon 1,12	2-methyl-2,4-pentanediol	0.5	128
nylon 1,5	1,4-butanediol	0.5	93
nylon 1,7[a]	water/dichloroacetic acid (5:1)	1.0	93

[a] From interfacial polymerization.

defined edges, as it is apparent from Figure 7. The reason for this behavior is not clear, perhaps a lower proportion of branched molecules or a molecular weight more favorable for regular folding of the chains.

Electron diffraction patterns from either isolated crystals or from the extremities of the sheaves confirms the single-crystal character of the laths. The patterns shown in Figure 7a–d are similar and present features similar to the conventional γ-form of nylon 6.[5] Four of the six inner spots have a spacing around 4.11–4.15 Å, and the other two have a spacing of 4.02–4.06 Å. Only two spots are visible in the 2.4-Å zone. They are located at right angles to the 4.02–4.06-Å spots and appear oriented along the growth direction of the crystals. The observed reflections and their indexes are summarized in Table 5. The *a*, *c*, and β parameters calculated from the observed *h0l* reflections are summarized in Table 8, together with the *b* parameters obtained by X-ray diffraction as described below. We can use either a primitive or a centered monoclinic unit cell. As will be discussed in the next paragraph, we prefer the centered cell according to the molecular symmetry. The *c* axis is always associated with the hydrogen bond direction and is parallel to the direction of maximum crystal elongation. In all cases the diffraction patterns indicate that the molecular chains are perpendicular to the basal crystal faces and are folded as a consequence of their molecular weight and the reduced lamellar thickness. The well-developed nyion 1,10 crystals were selected as most favorable for polyethylene decoration in order to ascertain the folding habit. The decoration shown in Figure 8 presents regular striations perpendicular to the long faces of the crystals. By analogy with polyethylene,[39] we interpret this as an indication that molecular chains are folded parallel to the long axis of the crystals and consequently along hydrogen-bonded sheets.

We have also studied two polyamides with n = odd. Nylon 1,5 crystallizes from 0.5% (w/v) 1,4-butanediol solutions at 93 °C as multilamellar aggregates in which a hexagonal habit is apparent (Figure 6e). The diameter of such aggregates can reach up to 1 μm with an individual lamellar thickness about 40 Å. All attempts to improve crystallization by changing solvent, temperature, or concentration were unsuccessful. Multilayered round/

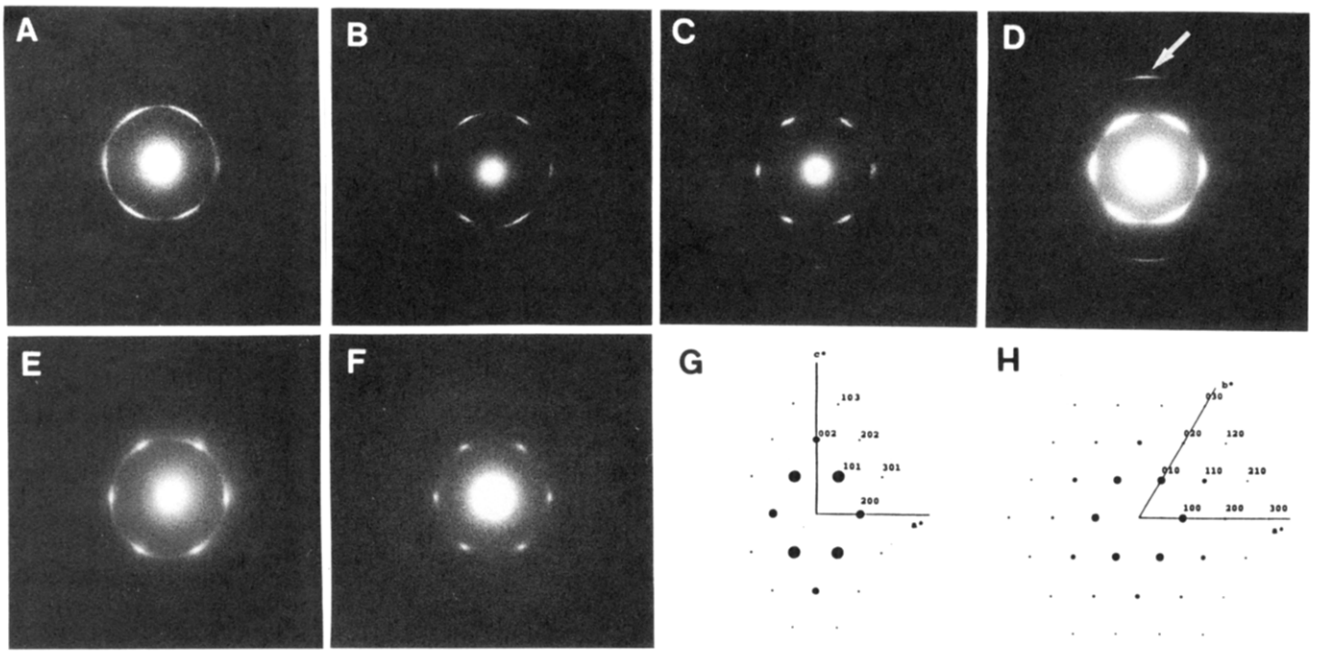

Figure 7. Selected area diffraction patterns from crystals of nylons (a) 1,6, (b) 1,8, (c) 1,10, (d), 1,12, (e) 1,5, and (f) 1,7. Drawings of the reciprocal net for nylons 1,*n* for (g) *n* = even, on the basis of a centered monoclinic cell, **c*** axis oriented parallel to the long axis of the crystals, and (h) *n* = odd, on the basis of an hexagonal lattice. When *n* = even the 002 reflection appears very clearly in all diagrams. In the figure this is more clearly seen in the more exposed pattern obtained from nylon 1,12, indicated by an arrow in (d).

Table 5. Measured and Calculated Electron Diffraction Spacings *d* (Å) for Nylons 1,*n*

	n even								*n* odd				
	nylon 1,6		nylon 1,8		nylon 1,10		nylon 1,12			nylon 1,5		nylon 1,7	
index[a]	measd[b]	calc	measd[b]	calc	measd[b]	calc	measd[b]	calc	index[c]	measd[b]	calc	measd[b]	calc
101	4.11 vs	4.11	4.14 vs	4.12	4.12 vs	4.12	4.15 vs	4.13	100	4.15 vs	4.15	4.15 vs	4.15
200	4.02 s	4.02	4.03 s	4.04	4.04 s	4.05	4.06 s	4.06	110	2.40 s	2.40		
002	2.40 m	2.40	2.41 m	2.40	2.42 m	2.40	2.42 m	2.40	200	2.07 m	2.07		
301	2.36 w	2.34		2.35	2.37 w	2.36		2.36	210	1.57 w	1.57		
202	2.06 w	2.06	2.07 w	2.06		2.06	2.07 w	2.06	300	1.38 w	1.38		
103	1.57 w	1.57		1.57	1.57 w	1.57	1.57 w	1.57					

[a] On the basis of the centered unit cells indicated in Table 8. [b] Abbreviations denote relative intensities: vs = very strong, s = strong, m = medium, w = weak. [c] On the basis of an hexagonal lattice with a = 4.79 Å.

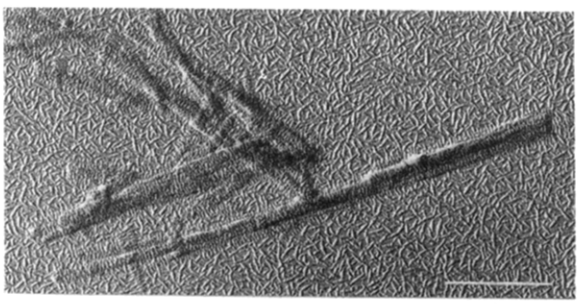

Figure 8. Electron micrograph of nylon 1,10 crystals grown at 70 °C from 2-methyl-2,4-pentanediol. The crystals are decorated with polyethylene using the Wittmann and Lotz[25] technique and shadowed with Pt/C at an angle of 15°. Scale bar: 1 μm.

hexagonal aggregates were always obtained. Round aggregates similar to those observed here have been previously reported in nylon 1,3[20] and in its isomer polygycline II.[40] These aggregates diffract like single crystals, exhibiting hexagonal diffraction with 6/*mmm* symmetry and a basic spacing of 4.15 Å (Figure 7e). Up to three orders of this reflection can be seen in the original pictures, which indicates that crystal structure is well preserved up to near 1-Å resolution. The pattern can be interpreted as corresponding to the normal projection along the chain axis of an hexagonal struture with a typical hydrogen-bonded interchain distance of 4.79 Å (Table 5). This hexagonal lattice is similar to the one reported for nylon 1,3[20] and indicates conformational differences between nylons 1,*n*, depending on the parity of *n*. This question will be discussed in the next section.

Crystallization of nylon 1,7 from diol solutions gave thick aggregates displaying a predominant circular shape. Unfortunately these aggregates were too thick to be examined by electron microscopy. Therefore we tried to crystallize nylon 1,7 by precipitation with water from dilute dichloroacetic acid solutions. Crystallization is completed in a few minutes after addition of five volumes of water. Polymers prepared by interfacial polymerization give better crystals than those prepared from formaldehyde, probably due to their greater regularity (Figure 6f,g). The morphology of the crystals was also highly dependent on the temperature used. The best crystals from interfacial samples were obtained at 93 °C as multilayered lath-shaped crystals (Figure 6g). The individual lamellae are about 1 μm long and not more than 0.3 μm wide. The crystals are thinner than in the other cases: the average thickness measured from shadowing is about 30 Å. Frequently lamellae overgrow in two or three directions at about 60° giving rise to cross-shaped figures. This feature may be interpreted as an epitaxial effect caused by a hexagonal or nearly hexagonal symmetry of the crystals. Selected area electron diffraction of the tips of aggregates gives an hexagonal pattern with six reflections at a basic spacing

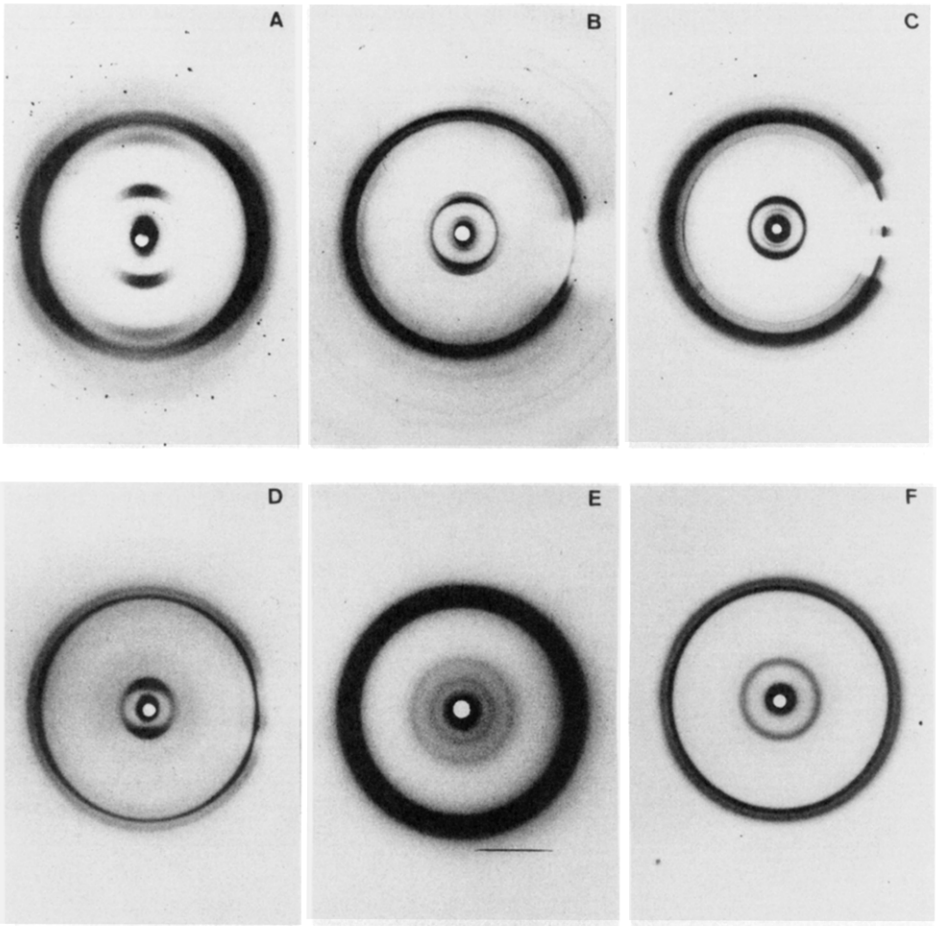

Figure 9. Wide-angle X-ray diffraction patterns from mats of sedimented crystals of nylons 1,*n*: (a) 1,6; (b) 1,8; (c) 1,10; (d) 1,12; (e) 1,5; (f) 1,7. The strong outer ring corresponds to the main equatorial spacings, whereas the inner ring corresponds to the molecular repeat. The latter ring becomes oriented in favorable cases (as in (a), for example). It also samples the lamellar spacing, as discussed in the text.

of 4.15 Å, as shown in Figure 7f. However individual crystals with a hexagonal shape were never observed. Thus, the crystals of nylon 1,7 are intermediate in character between those observed in nylon 1,5 and in nylons 1,*n* with n = even.

X-ray Diffraction. Unfortunately nylons 1,*n* cannot be oriented when a concentrated solution is stretched by standard laboratory procedures, probably due to the low molecular weight of the samples. Neither can fibers be prepared from the melt due to the observed decomposition near the melting point. As a consequence, only X-ray patterns from powders and from sedimented crystal mats were recorded.

In analogy with the electron microscope observations, different features were observed depending on n being odd or even. Nylons 1,*n* with n even have several common features (Figure 9a–d): (i) X-ray patterns of the crystal mats show partial orientation. (ii) A very strong reflection around 4.13 Å is observed. It is indexed as 101, in agreement with electron diffraction results. It encloses the weaker 200 reflection, which has a spacing of about 4.04 Å. These reflections are related to the lateral separation of chains. (iii) Several off-meridian arcs are observed which are useful for estimation of the chain axis repeat. The reflection around 3.88–3.97 Å is always the most intense. Its orientation is variable in different samples. This fact may be interpreted as a consequence of different degrees of order in the sedimentation of the narrow crystals. (iv) An intense diffuse ring associated with the periodicity along the chain and indexed as the 020 reflection is characteristic of powder diagrams. In mat patterns this reflection samples the lamellar thickness, indicating a regular thickness of the lamellar crystals. For example the 10.1 Å diffuse ring characteristic of the nylon 1,6 powder pattern is replaced by two sharp reflections at 11.4 and 9.3 Å, associated in this case with the fourth and fifth lamellar orders. (v) In mats, several lamellar orders are observed on the meridian. In all cases the first and second lamellar orders can be observed on low-angle X-ray diffraction patterns, and in a favorable case up to the sixth order was detected. A pattern obtained for nylon 1,6 is presented in Figure 10. The lamellar thickness is about 50 Å in all cases (Table 6), in agreement with electron microscopy observations and thus confirming chain folding. Table 6 summarizes the observed spacings and their indexes on the basis of the centered monoclinic unit cells given in Table 8. In all cases the repeat period along the chain (*b*-axis) is associated with two repeat units. The preliminary results reported for nylon 1,4[21] are fully consistent with those reported here for the higher members of the 1,*n* series. The calculated densities for these structures compare well with experimental values (Table 8). However these values are usually slightly lower than calculated probably due to some amorphous content in the samples, to chain folding, and to the low molecular weight of these samples.

With nylons 1,5 and 1,7 we could not obtain oriented mats. However the unoriented powder diagrams (Figure 9e,f) can be indexed (Table 7) on the basis of hexagonal lattices with a = 4.79 Å and c = 26.1 or 34.5 Å for nylons 1,5 and 1,7, respectively. Calculated densities agree with experimental values (Table 8). The powder patterns show

Table 6. Measured[a] and Calculated X-ray Diffraction Spacings *d* (Å) for Nylons 1,*n*

	nylon 1,6			nylon 1,8			nylon 1,10			nylon 1,12		
index[b]	measd[c]		calc	measd[c]		calc	measd[c]		calc	measd[c]		calc
lamellar thickness	46 s	M	46	55 s	M	55	48 vs	M	47	51 vs	M	50
2nd order	22.9 w	M	23	27.6 w	M	27.5	23 m	M	23.3	24 vw	M	25
3rd order							15.5 vs	M	15.7	16.4 vs	M	16.7
4th order	11.40 m	M	11.50	13.60 vs	M	13.75						
5th order	9.30 m	M	9.20	11.0 m	M	11.0						
6th order										8.28 m	M	8.33
020	10.10[d] s		10.10	12.6[d] vs		12.6	15.0[d] vs		15.0	17.8[d] vs	M	17.6
040	5.05 m	M	5.05							8.82 m	M	8.80
060										5.90 m	M	5.87
101	4.13 vs	E	4.11	4.13 vs	E	4.12	4.13 vs	E	4.12	4.13 vs	E	4.13
111			4.03			4.07			4.08			4.10
200			4.02			4.04			4.05			4.06
210	3.90 s	off M	3.94	3.96 s		3.99	3.97 s		4.01			4.03
121			3.81			3.91			3.97			4.02
220				3.87 w		3.85			3.91			
131	3.50 m	off M	3.51			3.70	3.81 w		3.81	3.88 s	off M	3.89
230			3.45	3.64 w		3.64			3.75			3.84
141			3.19			3.45			3.61			3.74
240	3.12 w	off M	3.14	3.40 m		3.40	3.52 m		3.56			
151			2.88	3.18 m		3.19	3.42 w		3.40	3.58 w		3.57
250	2.85 w		2.84			3.15			3.36			3.52
161			2.60	2.93 vw		2.94			3.18			3.38
260	2.59 w		2.58	2.86 m		2.91	3.14 m		3.15	3.36 w		3.35
171			2.36	2.70 w		2.71	3.02 m		2.97			
270	2.34 w		2.34	2.66 m		2.69						
181							2.80 m		2.77			3.02
280									2.75	2.99 w		2.99
191				2.30 s		2.31	2.62 m		2.59			
290						2.30	2.57 m		2.57	2.80 vw		2.82
1111							2.28 s		2.27	2.60 w		2.54
2110									2.26			
1131										2.27 s		2.27
2130												2.26
002	2.40 w	E	2.40	2.41 m	E	2.40	2.41 m		2.40	2.41 m	E	2.40
301			2.36			2.35			2.36			2.36

[a] Average values of spacings observed in low- and wide-angle X-ray pattern including powder and crystal mats. [b] On the basis of the centered unit cells indicated in Table 4. [c] Abbreviations denote relative intensities; vs = very strong, s = strong, m = medium, w = weak, and vw = very weak; and orientation of reflections, M = meridional, E = equatorial, and off M = off-meridional. [d] Observed as a diffuse ring only in powder patterns.

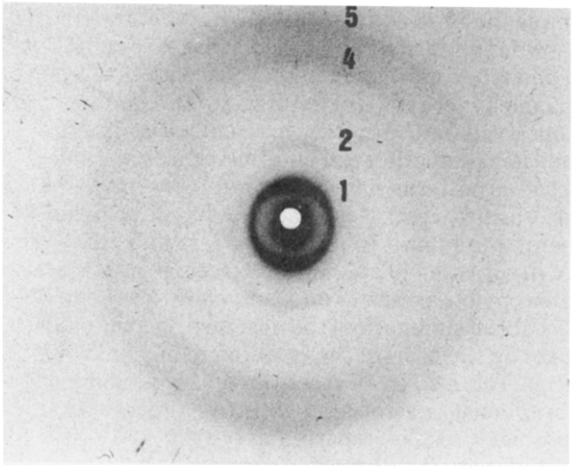

Figure 10. Low-angle diffraction pattern obtained from a crystal mat of nylon 1,6. The 1st, 2nd, 4th, and 5th orders of the lamellar spacing (46 Å) are clearly seen. The molecular repeat (10.1 Å) falls between the 4th and 5th orders of the lamellar spacing, which are thus enhanced.

Table 7. Measured[a] and Calculated X-ray Diffraction Spacings *d* (Å) for Nylons 1,5 and 1,7

nylon 1,5			nylon 1,7		
measd[b]	calc	index[c]	measd[b]	calc	index[d]
21.00 m	21.0	2nd order			
14.10 m	14.0	3rd order			
	8.40	5th order			
8.70 m	8.70	003	11.50 s	11.50	003
4.15 vs	4.15, 4.10	100, 101	5.75 m	5.75	006
3.75 s	3.75	103	4.15 vs	4.15, 4.11	100, 101
3.48 w	3.50	104	3.92 s	3.90	103
3.29 w	3.25	105	3.70 w	3.74	104
3.03 w	3.00	106	3.32 m	3.36	106
2.80 w	2.77	107	3.01 vw	2.99	108
2.56 w	2.56	101	2.77 m	2.81	109
2.41 m	2.40, 2.38, 2.38	110, 111, 109	2.53 vw	2.50	1010
2.28 m	2.31, 2.25	113, 114	2.40 w	2.40	110
			2.33 m	2.36, 2.35	1012, 113
			2.23 w	2.21	116

[a] Average values of spacings observed in low- and wide-angle X-ray patterns including powder and crystal mats. [b] Abbreviations denote relative intensities: vs = very strong, s = strong, m = medium, w = weak. [c] On the basis of a hexagonal lattice with a = 4.79 Å and c = 26.1 Å and a lamellar thickness of 42 Å. [d] On the basis of a hexagonal lattice with a = 4.79 Å and c = 34.5 Å.

the following relevant features. First, the prominent ring at about 4.15 Å fits well with electron diffraction data and corresponds to a hexagonal structure with an interchain distance of 4.79 Å. Second, the diffuse rings observed at 8.7 and 11.5 Å (for nylons 1,5 and 1,7, respectively) are interpreted as the third order of the axial structural repeat and correspond to the molecular repeat lengths. So 3-fold helices are assumed in order to explain the molecular structure. Third, reflections arising from the stacking of lamellae are only observed in wide- and low-angle X-ray diffraction patterns for nylon 1,5. The deduced lamellar thickness of 42 Å is in full agreement with electron

Table 8. Summary of the Main Crystallographic Data for Nylons 1,*n*[a]

	a (Å)					*β* (deg)			density (g L^{-1})	
polymer	primitive unit cell	centered unit cell	*b* (Å)	*c* (Å)	*α* (deg)	primitive unit cell	centered unit cell	*γ* (deg)	exptl[b]	calc
nylon 1,6	4.68	8.04	20.2[c]	4.79	90	120.8	90	90	1.29	1.33
nylon 1,8	4.70	8.08	25.2[c]	4.79	90	120.7	90	90	1.24	1.25
nylon 1,10	4.71	8.10	30.0[c]	4.79	90	120.6	90	90	1.17	1.21
nylon 1,12	4.71	8.12	35.2[c]	4.79	90	120.5	90	90	1.12	1.16
nylon 1,3[d]	4.79		4.79	18.0[c]	90	90		120	1.53	1.58
nylon 1,5	4.79		4.79	26.1[c]	90	90		120	1.31	1.36
nylon 1,7	4.79		4.79	34.5[c]	90	90		120	1.23	1.24

[a] Parameters related to the chain packing were determined from electron diffraction data, and the remaining ones, from X-ray diffraction data. [b] Measured by flotation of powder samples in mixtures of ethanol and carbon tetrachloride. [c] Fiber identity period. *b*-axis for a monoclinic lattice and *c*-axis of a hexagonal lattice. [d] Data of Puiggalí *et al.*[20]

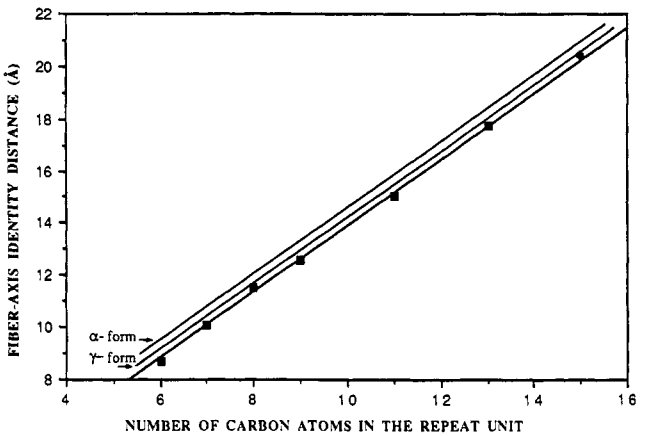

Figure 11. Unit repeat length of nylons 1,*n* versus number of carbon atoms in the repeat unit. Average values for the conventional *α* and *γ* forms are also indicated.[2]

microscopy observations. No lamellar orders have been observed in X-ray patterns of nylon 1,7. This fact may be due to irregular lamellar thickness or a poor stacking of the very thin lamellae in mats. Since the lamella are very thin (about 30 Å), they can rarely accommodate the assumed repeat period (34.5 Å) within its reduced thickness. The observed "starfish" morphology of these crystals (Figure 6g) may be due to this fact. It cannot be excluded that crystals of this material only develop two hydrogen bond directions within each thin lamella instead of the three equivalent ones expected for a true hexagonal lattice.

The unit repeat lengths for all the nylons studied here are shorter than those deduced by extrapolation of other nylons in the *α* or *γ* forms.[36] This is an additional indication that we are dealing with a new nylon structure. Figure 11 shows a linear relationship between the experimental repeat length and the number of carbon atoms in the repeat unit. A constant shortening of about 0.2–0.3 Å with respect to the *γ*-form and about 0.5–0.6 Å with respect to the *α*-form is found.

Finally, we mention that a weak and variable reflection, depending on the crystallization conditions, may be observed in some samples in the equatorial region at about 4.4–4.7 Å spacing. This reflection cannot be indexed on the basis of the proposed unit cells. We interpret this observation as due to a small amount of a different structure, probably related to a conventional *α* form.

Molecular Structure of Lamellar Crystals. As shown in the previous sections, the polymers studied here have a rather low molecular weight. Nevertheless they never give rise to crystals containing the fully extended molecules, at least under the crystallization conditions used here. As shown in Table 9, they fold once or twice in order to form the lamellar crystals. As a result of this limited amount of folding, end groups should be an important component of the crystals, probably located at

Table 9. Molecular Parameters for Lamellar Crystals

nylon	*l*, lamellar thickness (Å)	*R*[a]	no. of stems[b]
1,5	42	4.83	3.3
1,6	46	4.55	3.1
1,7	~30		
1,8	55	4.37	3.0
1,10	47	3.13	2.5
1,12	50	2.84	2.1

[a] $R = l/m$ is the number of monomer units which span a lamellar crystal, where m is the length of a monomer unit calculated from the values given in Table 8. Thus $m = b/2$ for n = even and $m = c/3$ for n = odd. [b] This column gives the average number of stems of each individual polymer molecule in a lamellar crystal. It is obtained by dividing the average degree of polymerization x_n (given in Table 1) by R, given in the previous column.

the surface of the lamellae. This fact seems to imply a considerable degree of imperfection in the crystals, but surprisingly the lamellae have a rather constant thickness in each case, as demonstrated by the fact that five to six orders of the lamellar spacings can be detected in some low angle pictures, as shown in Figure 10 and in Table 6.

Inspection of Table 9 shows some clear patterns in the lamellar crystals obtained from these polyamides: (1) The lamellar thickness does not vary much in the different nylons studied, between 42 and 55 Å. Nylon 1,7 appears to form thinner lamellae, but their thickness could not be determined with accuracy by X-ray diffraction. (2) As a result, the number of monomer units *R* within a lamellar thickness decreases as *n* increases, so that nylon 1,5 has 4.83 repeats and nylons 1,10 and 1,12 have about 3 repeats. The equivalent number of hydrogen bonds decreases from 9 to 10 in nylon 1,5 to 6 in nylon 1,12. This trend had already been reported by Dreyfuss[41] in his survey of polyamides, although in the 1,*n* family the values of *R* are comparatively smaller. (3) The molecular weight of the samples apparently does not have a determining influence on the results just discussed, since it varies between 1390 and 2350 in the various samples studied. As shown in Table 9 the number of folds in each polymer varies, probably in order to accommodate the most stable number of monomer units within the lamellar thickness. (4) Since there are strong hydrogen bonds in each unit cell, it would be expected that for regular folding the number of monomer units in one lamellae should be a whole number, but this is not observed, as shown in Table 9. Such discrepancy might be due to the small size of these polymers and the influence of terminal groups in the folding. Nevertheless it is striking that the lamellae apparently have a very regular thickness.

In summary, the nylons 1,*n*, which have a small but rather variable molecular weight, have lamellae with a rather constant thickness. It cannot be excluded that during crystal growth there is a selection of molecules according to their size, so that the molecules within a crystal

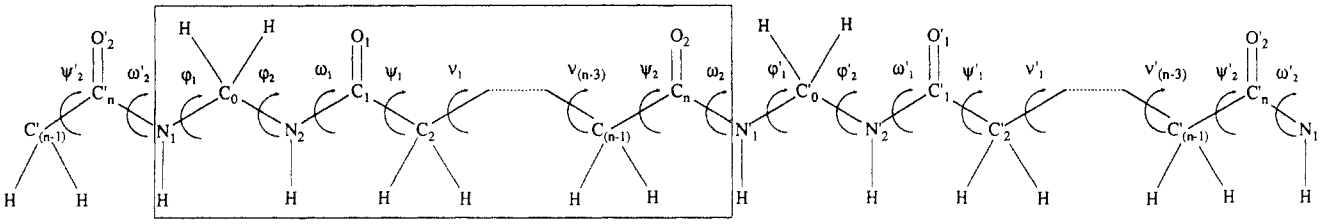

Figure 12. Representation of a generic nylon 1,*n* backbone showing atom numbering and definition of torsional angles. The numbering is according to the chemical repeat unit whereas in Table 10 we join the torsional angles according to the crystallographic unit.

Table 10. Conformational Parameters and Hydrogen Bond Geometry for the Models of Nylon 1,5 and 1,6

	nylon 1,5	nylon 1,6
molecular sym	3_22	$2/b$
space group	$P3_212$	$B2/b11$
torsional angles (deg)		
φ_1	+88.0	+87.5
ψ_1	−157.4	−120.0
ψ'_2	−157.4	−120.0
φ_2	+88.0	+87.5
φ'_1	+88.0	−87.5
ψ'_1	−157.4	+120.0
ψ_2	−157.4	+120.0
φ'_2	+88.0	−87.5
ω_i, ω'_i	180.0	180.0
ν_i, ν'_i	180.0	180.0
hydrogen bond geometry		
d(H···O) (Å)	1.87	1.86
d(N···O) (Å)	2.82	2.82
∠NHO (deg)	159.0	158.0

might have a rather sharp distribution of molecular weights.

Structural Models. The experimental data for nylons 1,5 and 1,6 have been used for structural modeling as representative of nylons 1,*n* with *n* odd and *n* even. The structural investigation of both polymers have been carried out with the LALS (linked-atom least-squares) program.[30] The description of a generic residue of nylon 1,*n* is given in Figure 12. Standard bond distances and bond angles for polyamides were adopted to build the repeat unit. The torsional angles ω_i and ν_i were kept in the trans-conformation as is usual in polyamides. So only the four torsional angles next to the amide groups (φ_i and ψ_i) and the positional parameters which fix the chain in the unit cell were needed to define the chain conformation and packing. The models were refined using as constraints the unit cell dimensions and the optimum hydrogen bond geometry. X-ray and electron diffraction data were used to test and improve the quality of the models. An isotropic temperature factor $\exp[-B((\sin\theta)/\lambda^2)]$ with $B = 5$ Å^2 was used throughout all the refinement process.

In the proposed model for nylon 1,6 the values of the torsional angles φ_i (Table 10) are close to those observed[18] and calculated[19] for some methylene diamides, whereas the dicarboxylic moiety assumes a conformational arrangement $s^-t_4s^+$ similar to that found in the γ form of nylons.[2] Quantum mechanical studies of the model molecule bis(acetamido)methane provide two enantiomeric minima with the same energy when the torsional angles are $\varphi_1 = \varphi_2 = 80$ or $-80°$.[19] This molecule has recently been analyzed by single-crystal X-ray diffraction, and similar experimental values are found[18] ($\varphi_1 = \varphi_2 = 85.1°$). The shortening observed in the chain repeat lengths is justified by this particular conformation, where close amide groups are oriented in exactly opposite directions allowing a single hydrogen bond direction as is inferred from electron micrographs. Molecular chains have a center of symmetry in the middle of the $-(CH_2)_4-$ methylene segment and a binary axis perpendicular to the chain direction through isolated methylene groups. This molecular symmetry ($2/b$) has the consequence that equivalent torsional angles in consecutive repeat units are equal but with opposite sign. Furthermore the expected adirectional configuration of the polymer chains is preserved. A space group $B2/b11$ is compatible with molecular symmetry, with the systematic absences on X-ray patterns (i.e., reflections $0k0$ for k = odd), and also with the $2/mmm$ symmetry of the $h0l$ electron diffraction patterns. The model also appears stereochemically suitable and shows no significant contacts. All hydrogen bonds are formed with length and angle values within the standard ranges (Table 10).

Molecular drawings of lateral and equatorial projections of the molecular arrangement are shown in Figure 13. The atomic coordinates used in the final intensity calculations are summarized in Table 11. Only the coordinates of one asymmetric unit, half the unit repeat, are given because the structure is fully described taking into account the space group. The observed and calculated structure factors of the reflections used in the X-ray diffraction analysis are given in Table 12 and 13. In some cases several hkl planes contribute to the calculated structure factors due to the similarity in their spacings. An acceptable agreement between observed and calculated data is attained, with no large discrepancies for any particular reflection. The disagreement R-factors ($\sum|F_o - F_c|/\sum F_o$) for X-ray and electron diffraction analysis were 14.1 and 14.4, respectively.

A similar model, but with a 3-fold helix for nylon 1,5 can be generated if we change the conformation of the polymethylene segment while preserving the conformation around the central methylene group. The main differences with the 1,6 model is that all residues have the same conformational angles instead of alternatively changing sign. In order to optimize the hydrogen bond parameters and van der Waals contacts, the ψ angles became slightly different in both cases. In nylon 1,5 a 3-fold helix is generated with $\psi_1 = \psi_2 = -157°$, which produces a rotation between the C–O directions, while the torsional angles of the methylene diamide are kept in their low-energy value ($\varphi_1 = \varphi_2 = 80 \pm 10°$). Such conformational angles are practically identical with those found in Polyglycine II,[42] which also forms a 3-fold helix. Quantum mechanical calculations confirm[43] that this conformation is energetically stabilized for nylons 1,*n* with *n* odd. The proposed crystal structure consists of an hexagonal array of 3-fold helices interlinked by a three-dimensional network of hydrogen bonds (Figure 13b,d). The distances and angles calculated for hydrogen bonds (given in Table 10) are within the permissible range. Torsional angles for left-handed helices are also given in Table 10. As there are no asymmetric carbon atoms, right-handed helices are equally probable, with all equivalent torsional angles with inverted signs. However only helices with the same sense can be present within a given crystal, in order to enable the formation of all hydrogen bonds. The binary axis perpendicular to the chain axis through the isolated methylene and through the middle of the $-(CH_2)_4-$ segment keeps

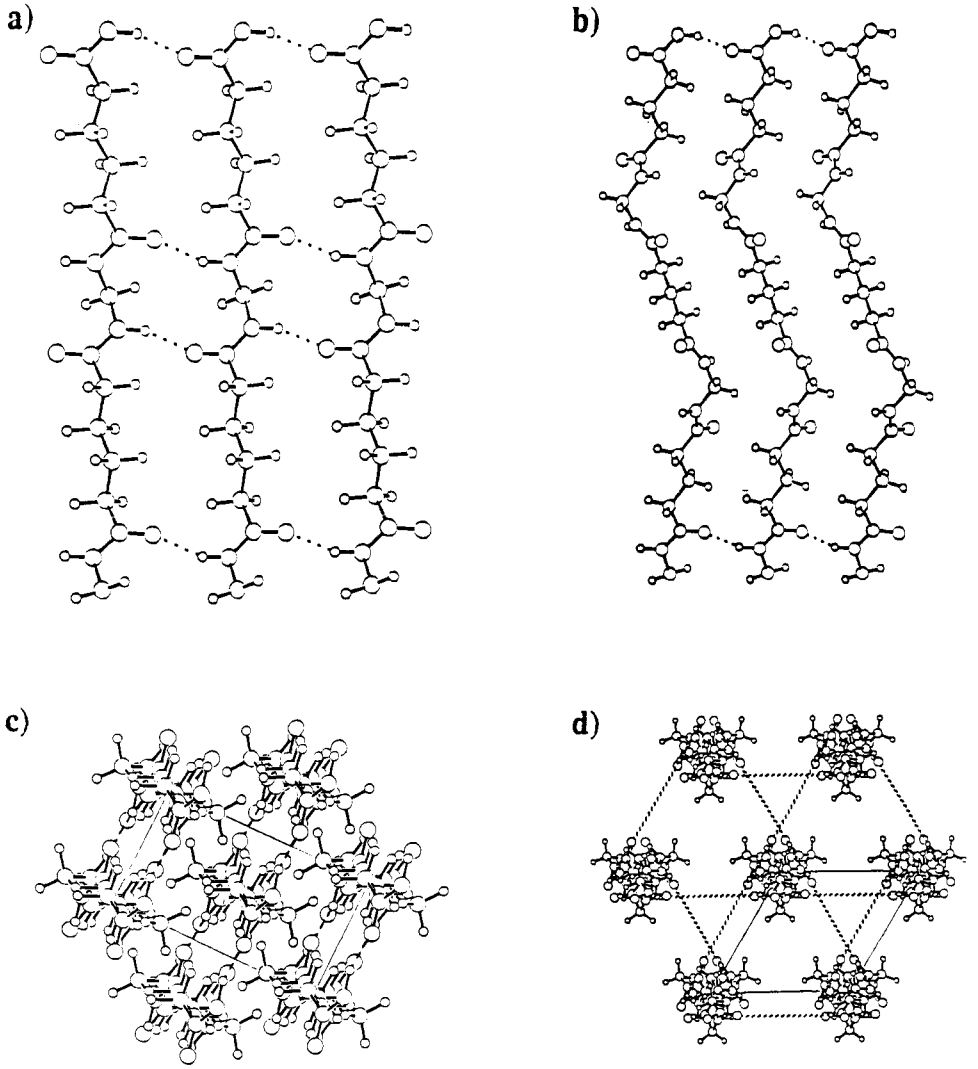

Figure 13. Hydrogen bonding (dashed lines) between three neighboring chains (side view) of nylons 1,6 (a) and 1,5 (b) and equatorial projections of a centered molecule and its six surrounding neighbors for nylons 1,6 (c) and 1,5 (d). In the last case the molecular chains have been drawn with an increased separation between them in order to show hydrogen bonds more clearly. In (c) and (d) the unit cell is indicated with a thinner line.

Table 11. Fractional Coordinates[a] for the Models of Nylons 1,5 and 1,6 (Molecular Axis at $x = 0$, $y = 0$)

nylon 1,5				nylon 1,6			
atom[b]	x	y	z	atom[b]	x	y	z
C_0	−0.30867	0.30932	−0.05118	C_0	0.89496	−0.61799	0.89746
H_1C_0	−0.21115	0.55956	−0.03979	H_1C_0	1.04660	−0.63213	1.15267
N_2	−0.27480	0.13034	−0.00934	N_2	0.68372	−0.56232	0.86648
HN_2	−0.44364	−0.09970	−0.00820	HN_2	0.62367	−0.55938	1.04091
C_1	−0.03298	0.26651	0.02401	C_1	0.57846	−0.51870	0.62508
O_1	0.18485	0.54796	0.02255	O_1	0.65223	−0.52246	0.41293
C_2	−0.05200	0.05772	0.06898	C_2	0.35943	−0.46317	0.62413
H_1C_2	−0.30154	−0.09250	0.08092	H_1C_2	0.32453	−0.46888	0.83109
H_2C_2	0.04500	−0.09494	0.05729	H_2C_2	0.11705	−0.46489	0.39917
C_3	0.14706	0.27237	0.11407	C_3	0.52835	−0.39608	0.64861
H_1C_3	0.05015	0.42504	0.12581	H_1C_3	0.77071	−0.39430	0.87358
				H_2C_3	0.56322	−0.39031	0.44166

[a] According to the primitive unit cells indicated in Table 8. [b] Atom numbering as in Figure 12.

the adirectional configuration of molecular chains. The $P3m1$ symmetry of the c-axis projection is consistent with the $6/mmm$ symmetry exhibited by the $hk0$ electron diffraction patterns. The crystal structure in space group $P3_212$ or $P3_112$ is confirmed by the structure factor calculations (Table 12 and 13). Acceptable R-factors are obtained for X-ray diffraction data ($R = 21.2$) and also for electron diffraction data ($R = 15$). Table 11 presents the atomic coordinates of the asymmetric unit used for calculations.

We should stress that the angles (Table 10) and coordinates (Table 11) estimated for our models are only approximate, since only 10 experimental diffraction intensities could be determined (Table 12). With such a small number of data, our refinement can only give approximate values. On the other hand, there is little doubt that nylons 1,n have a unique conformation which differs from that of other polyamides. It is based on the structure of monomethylene bis(amide) units, for which low molecular weight models[18] and theoretical calcula-

Table 12. Observed (F_o) and Calculated (F_c) X-ray Structure Factors for the Models of Nylons 1,5 and 1,6

nylon 1,5 (R_f = 21.2%)							nylon 1,6 (R_f = 14.1%)						
ring	d(obs) (Å)	F_0	hkl	d(cal) (Å)	m^a	F_c^b	ring	d(obs) (Å)	F_0	hkl	d(cal) (Å)	m^a	F_c^b
1	8.7	19	003	8.70	1	20	1	10.1	17	020	10.1	1	18
2	4.15	91	100	4.15	3	76	2	5.05	31	040	5.05	1	18
			101	4.10	6								
			102	3.95	6								
3	3.75	49	103	3.75	6	30	3	4.13	91	101	4.11	2	92
										111	4.03	4	
										200	4.02	1	
4	3.48	16	104	3.50	6	21	4	3.90	74	210	3.94	2	73
										121	3.81	4	
5	3.29	25	105	3.25	6	18	5	3.50	41	131	3.51	4	47
										230	3.45	2	
6	3.03	47	106	3.00	6	43	6	3.12	52	141	3.19	4	29
										240	3.14	2	
7	2.80	22	107	2.77	6	16	7	2.85	41	151	2.88	4	15
										250	2.84	2	
8	2.56	30	108	2.56	6	45	8	2.59	20	161	2.60	4	43
										260	2.58	2	
9	2.41	51	110	2.40	3	44	9	2.40	26	002	2.40	1	27
			111	2.38	6								
			109	2.38	6								
10	2.28	80	113	2.31	6	93	10	2.34	46	171	2.36	4	55
			114	2.25	6					270	2.34	2	

[a] Multiplicity. [b] Calculated as $F_c = (\sum m_{hkl} F_{c\,hkl}^2)^{1/2}$.

Table 13. Observed (F_o) and Calculated (F_c) Electron Beam Structure Factors for the Models of Nylons 1,5 and 1,6

nylon 1,5 (R_f = 18.8%)						nylon 1,6 (R_f = 14.4%)					
d(obs) (Å)	F_o^a	hkl	d(calc) (Å)	m^b	F_c	d(obs) (Å)	F_o^a	hkl	d(calc) (Å)	m^b	F_c
4.15	8.7	100	4.15	3	8.7	4.11	9.6	101	4.11	2	10.0
2.40	4.0	110	2.40	3	4.6	4.02	4.4	200	4.02	1	3.2
2.07	3.0	200	2.07	3	2.7	2.40	2.8	002	2.40	1	2.6
1.57	2.0	210	1.57	6	1.8	2.36	1.8	301	2.34	2	1.4
1.38	1.0	300	1.38	3	3.6	2.06	1.8	202	2.06	2	1.2
						1.57	1.8	103	1.57	2	2.0

[a] All equivalent spots have a similar intensity. [b] Multiplicity.

tions[19] predict the conformation used in our models. Furthermore the electron microscopy results confirm that we are in the presence of a unique conformation, which is different from conventional nylons.

Nylon 1,7 could have a structure similar to nylon 1,5, but it cannot be excluded that a slightly different conformation may appear as the number of methylene units increases. In fact polyglycine II,[42] nylon 1,3,[20] and nylon 1,5 have all similar conformations with 3-fold helices. In the case of nylon 1,7 a thinner lamellar structure has been found, together with a different crystal morphology. It cannot be excluded that in this case another related conformation appears, perhaps with only two hydrogen bond directions, as found in the case of nylons n,3.[14] A study of nylons 1,n with a larger number of methylene units could help to resolve this question.

Conclusions

The results of the present study can be summarized as follows: (1) The conformation of crystalline nylons 1,n differs from the conventional α and γ forms of most polyamides. (2) The unique conformation of these polymers gives them a much higher structural stability (high T_m) than found in conventional nylons. On the other hand, their chemical stability is comparatively low since decomposition starts at about 230 °C. (3) The isolated methylene group placed between two amide residues has strong conformational preferences. As a result the two neighboring amide groups are oriented in opposite directions. (4) Conformational differences have been found as a function of the number of methylene groups in the chain. These differences may be interpreted as a consequence of conformational changes in the dicarboxylic moiety depending on the parity of the number of methylene groups. (5) Packing of the chains is monoclinic when n is even and the structure is defined by a $B2/b11$ space group. A single hydrogen bond direction is present, and the fold plane corresponds to the plane of hydrogen bonds. (6) Molecular chains are packed in an hexagonal array when n is odd and has a low value. The structure is defined by a $P3_212$ or $P3_112$ space group depending on helix sense. Three hydrogen bond directions are present in this case, and each helix is hydrogen bonded with its six neighboring helices. (7) Molecular chains are folded within the lamella. The folding takes place along the hydrogen-bonded sheets for nylon 1,10 and probably also in all nylons 1,n with n even.

Acknowledgment. This work has been carried out under Contract No. BE-3106-89 with the CEE through the BRITE/EURAM program. Further support has been received by a CIRIT-CICYT Grant No. QFN 91-4204. We are thankful to Drs. J. M. Fernández and I. Fita for helpful discussions. L.F. acknowledges financial support from the Ministerio de Educación y Ciencia. E.N. acknowledges financial support from the Department d'Ensenyament de la Generalitat de Catalunya.

References and Notes

(1) Holmes, D. R.; Bunn, C. W.; Smith, D. J. *J. Polym. Sci.* **1955**, *17*, 159.
(2) Kinoshita, Y. *Makromol. Chem.* **1959**, *33*, 1.
(3) Vogelsong, D. C. *J. Polym. Sci., Part A: Gen. Pap.* **1963**, 1055.
(4) Cogazzi, G.; Fichera, A.; Malta, V.; Zannetti, R. *Makromol. Chem.* **1978**, *179*, 509.

(5) Kyotani, M.; Mitsubishi, S. *J. Polym. Sci., Polym. Phys. Ed.* **1972**, *10*, 1492.
(6) Miyasaka, K.; Ishikawa, K. *J. Polym. Sci., Polym. Chem. Ed.* **1967**, *5*, 3017.
(7) Arimoto, H. *J. Polym. Sci., Part A: Gen. Pap.* **1964**, *2*, 2283.
(8) Fraser, R. D. B.; Mcrae, T. P. *Conformation in fibrous protein and related polypeptides*; Academic Press: New York, 1973.
(9) Puiggalí, J.; Muñoz-Guerra, S.; Lotz, B. *Macromolecules* **1986**, *19*, 1119.
(10) Puiggalí, J.; Muñoz-Guerra, S.; Subirana, J. A. *Polymer* **1987**, *28*, 209.
(11) Muñoz-Guerra, S.; Fita, I.; Aymamí, J.; Puiggalí, J. *Macromolecules* **1988**, *21*, 3464.
(12) Puiggalí, J.; Muñoz-Guerra, S. *J. Polym. Sci., Part B: Polym. Phys.* **1989**, *27*, 1563.
(13) Bella, J.; Puiggalí, J.; Subirana, J. A. *Polymer* **1994**, *35*, 1231.
(14) Aceituno, J. E.; Subirana, J. A. Electron Microscopy. In *EUREM 92*; López-Galindo, A., Rodriguez-García, M. I., Eds.; Publicaciones de la Universidad de Granada: Granada, 1992; Vol. 2, p 375.
(15) Puiggalí, J.; Aceituno, J. E.; Franco, L.; Lloveras, J.; Prieto, A.; Vidal, X.; Xenopoulos, A.; Fernández-Santín, J. M.; Subirana, J. A. *Prog. Coll. Polym. Sci.* **1992**, *87*, 35.
(16) Tereshko, V.; Navarro, E.; Puiggalí, J.; Subirana, J. A. *Macromolecules* **1993**, *26*, 7024.
(17) Magat, E. E.; Chandler, L. B.; Faris, B. F.; Reith, J. E.; Salysbury, F. L. *J. Am. Chem. Soc.* **1951**, *73*, 1031.
(18) El-Masdouri, L.; Aubry, A.; Gómez, E.; Vitoux, B.; Marraud M. *Acta Crystallogr., Sect. C* **1992**, 176.
(19) Alemán, C.; Pérez, J. J. *J. Mol. Struct. (THEOCHEM)* **1994**, *304*, 17.
(20) Puiggalí, J.; Muñoz-Guerra, S. *J. Polym. Sci., Part B: Polym. Phys.* **1987**, 513.
(21) Puiggalí, J.; Muñoz-Guerra, S.; Subirana, J. A. *J. Polym. Sci., Part A: Polym. Chem.* **1987**, 1445.
(22) Walker, I. *Formaldehyde*; Reinhold: New York, 1944; p 207.
(23) Riddick, J. A.; Bunger, W. B. *Organic Solvents*; Wiley Interscience: New York, 1970.
(24) Mowry, D. T.; Ringwald, E. L. *J. Am. Chem. Soc.* **1950**, *72*, 4439.
(25) Franco, L.; Aceituno, J. E.; Subirana, J. A.; Puiggalí, J. *Polym. Prepr.* **1992**, *31*, 325.
(26) Sorenson, W. R.; Campbell, T. W. *Preparative Methods of Polymer Chemistry*; Interscience: New York, 1961.
(27) Radhakrishna, A. S.; Darham, M. E.; Riggs, R. M.; Loudon, G. M. *J. Org. Chem.* **1979**, *10*, 1746.
(28) Wittmann, J. C.; Lotz, B. *J. Polym. Sci., Polym. Lett. Ed.* **1985**, *23*, 200.
(29) Whittaker, E. J. W. *Acta Crystallogr.* **1953**, *6*, 222.
(30) Campbell-Smith, P.; Arnott, S. *Acta Crystallogr., Sect A* **1978**, *34*, 3.
(31) Elias, H. G.; Schumacher, R. *Makromol. Chem.* **1964**, *76*, 23.
(32) Abu-Isa, I. *J. Polym. Sci., Polym. Chem. Ed.* **1971**, *9*, 199.
(33) Xenopoulos, A.; Wunderlich, B.; Subirana, J. A. *Eur. Polym. J.* **1993**, *29* (7), 927.
(34) Wunderlich, B. *Macromolecular Physics*; Academic Press: New York, 1980; Vol. 3.
(35) Champetier, G.; Monnerie, L. *Introduction à la chimie macromoléculaire*; Masson et cie. editeurs: Paris, 1969.
(36) Miller, R. L. *Polymer Handbook*, 3rd ed.; Brandrup, J., Immergut, E. H., Eds.; Wiley Interscience: New York, 1989; Chapter VI.
(37) Bella, J.; Subirana, J. A. *Polym. Prepr.* **1992**, *31*, 276.
(38) Wendoloski, J. J.; Gardner, K. H.; Hirschinger, J.; Miura, H.; English, A. B. *Science* **1990**, *247*, 431.
(39) Organ, S.; Keller, A. *J. Polym. Sci., Part B: Polym. Phys.* **1987**, *25*, 2409.
(40) Padden, F. J., Jr.; Keith, H. D. *J. Appl. Phys.* **1965**, *36*, 2987.
(41) Dreyfuss, P. *J. Polym. Sci., Polym. Phys. Ed.* **1973**, *11*, 201.
(42) Crick, F. H. C.; Rich, A. *Nature* **1955**, *176*, 780.
(43) Alemán, C.; Franco, L.; Puiggalí, J. *Macromolecules*, in press.